

Simulation of Everting Tube Experiments

Blake Hannaford
July 12, 2024

1 Introduction

1.1 Literature Review

Prior studies of eversion mechanics have relied on the assumption of constant pressure over time and throughout the extent of the device. [1] Applied biomechanical models for plant shoot growth to analogous physical processes in everting tubes and combined it with experimental measurements. Notably, for their speeds and design parameters, they did not find an effect of air flow drag caused by filling the everting tube. [?] Performed mostly quasi-static modeling of ETs but studied the important buckling phenomena in complex geometric environments. [2] created a dynamic, lumped parameter mechanical model of eversion with special emphasis on friction properties between an everting tube and its environment as well as a second contact between the tube and a rod (catheter) in contact with the everted material.

1.2 Observed Eversion Characteristics

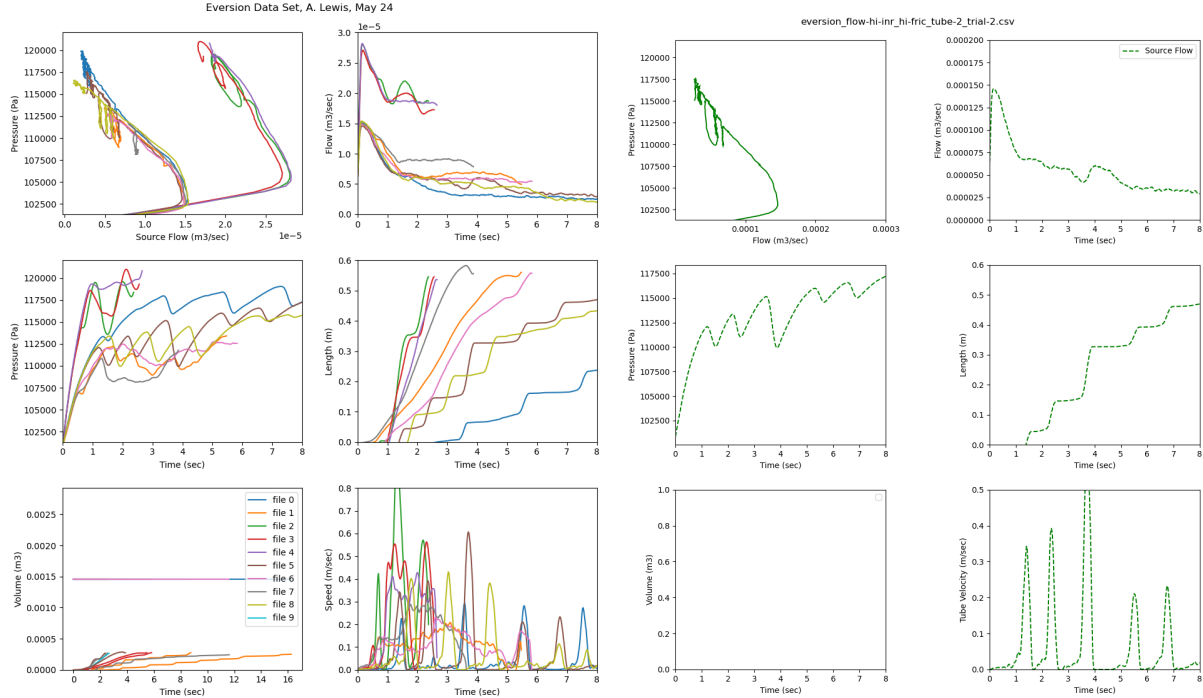


Figure 1: Experimental data displaying dynamic characteristics of loaded eversion. All data (Left), single example (Right) (See Lewis, Fig 9. Loads: high inertia, high Friction)

Some theory of everting tubes has been reviewed above. Complex dynamic behaviors of a tube everting inside a straight tube of approximately the same diameter as the inflated tubing material were measured by Lewis [?] (Figure 1, Left panel). One experiment which displays several interesting everting characteristics is shown in Figure 1, Right Panel.

Referring first to the length-vs-time plot (middle right), we see a start-stop or staircase behavior sometimes seen with eversion under relatively constant input pressure. It should be noted that this particular eversion experiment was loaded by reel inertia and by friction applied to the reel. Velocity (lower right) indicates a series of peaks where the eversion “breaks-free” but then stops again a short time later.

Pressure (middle left) first grows for about 1 second without corresponding eversion motion, and then oscillates in approximate synchrony with the velocity peaks.

Finally, the pressure-flow phase plot (top left) shows diagonal slope (the trajectory proceeds from lower right (high initial flow with low pressure) to upper left (lower flow, higher pressure). The trajectory makes loops to lower pressures and back up to the slope at higher pressures. These loops correspond in time to the pressure oscillations (middle left).

These dynamic characteristics (start-stop bursting, pressure oscillations, diagonal phase trajectory, and downward loops) were not all present under all experimental conditions.

1.3 Simulation Goals

The goals of this simulation are:

1. Increase fundamental understanding of the eversion process.
2. Identify key parameters capable of representing the complex dynamic characteristics above.
3. Identify values and value ranges for unknown parameters which fit individual experiments.
4. Clearly segregate the parameters into known, measured quantities vs. free parameters.
5. Codify an efficient manual method for parameter identification.

1.4 Dynamic Model

The dynamic model of an eversion drive system includes;

- An everting tube of length L and growth rate \dot{L} .
- A pressurized housing
- A reel with rotation $\theta, \dot{\theta}, \ddot{\theta}$, on which tubing is rolled having inertia (assume fixed) of J and radius r .
- A brake which applies a Coulomb friction torque to the reel

$$\tau_c = C \text{sgn}(\dot{\theta})$$

- A “crumple zone” in which eversion material can accumulate between the reel and the everting tube. The length of material in the crumple zone is L_c .
- Eversion happens when the eversion force (pressure \times face area of the tube) exceeds any retarding forces.
- Forces which can oppose eversion include,
 - drag forces inertial forces required to pull the tubing material inside the deployed tube,
 - reel inertia and reel friction resulting from unspooling material,

The everting tube can be in one of two states:

- GROWING (the tube is actively everting, $\dot{L} > 0$)
- STUCK (the tube is not growing due to insufficient everting force, $\dot{L} = 0$)

and the reel/crumple zone can be in one of two additional states:

- TAUGHT (the crumple zone has zero length, $L_c = 0$)
- SLACK (there is material in the crumple zone, $L_c > 0$)

Together the system can be in four states comprising the permutations of these two state variables.

2 System Equations:

After setting initial conditions (see below), we model eversion dynamics by:

1. Computing pressure, volume, and flow from the source.
2. Computing forces applied to the eversion tip.
3. Accounting for the mechanical advantage (everting material speed is $2 \times \dot{L}$, Pressure applied to everting front develops 1/2 the everting force expected from $P \times A$.)
4. Selecting the dynamic mode from the four combined states above. GROWING and STUCK are selected by force thresholds applied to net eversion force. TAUGHT and SLACK are selected by checking length of the crumple zone material.
5. According to the dynamic mode, summing forces, equating to zero, solving for tube and reel accelerations.
6. Eversion does not come to an instant halt. We empirically model exponential decay of velocity as tube decelerates.

Specifically:

$$V_t = V_{housing} - V_{contents} + LA \quad (1)$$

V_t includes both the reel housing minus the volume of its contents, and the everted tube of length L with cross sectional area A .

From the ideal gas equation:

$$P = \frac{NRT}{V_t} \quad (2)$$

where N is the molar mass of gas in the system, R is the gas constant, and T is the temperature in °K, (which we assume is constant).

Computing Forces:

$$F_{ever} = \max(0, PA/2) \quad (3)$$

$$F_c = \tau_{Coulomb}/r \quad (4)$$

Coulomb friction is independent of velocity so does not get scaled by the $2 \times$ mechanical advantage.

Computing acceleration according to the dynamic state:

GROWING and SLACK:

$$\ddot{L} = \frac{F_{ever} - F_D(L, \dot{L}) - F_C}{M_T} \quad (5)$$

$$\dot{\theta} = \tau_{Coulomb}/J \quad (6)$$

GROWING and TAUGHT:

$$\ddot{L} = (F_{ever} - F_D - F_C)/(M_T + J/r^2) \quad (7)$$

$$\ddot{\theta} = \ddot{L}/r \quad (8)$$

STUCK and (SLACK or TAUGHT):

$$\ddot{L} = -1 * (\max)(0, \alpha * \dot{L}) \quad (9)$$

$$\ddot{\theta} = \tau_{Coulomb}/J \quad (10)$$

where α is an empirical time constant modeling the dynamics of eversion stopping.

Modeling flow from the pressure source (Thevenin equivalent):

$$Fl_{source} = \frac{P_{source} - P}{R_{source}} \quad (11)$$

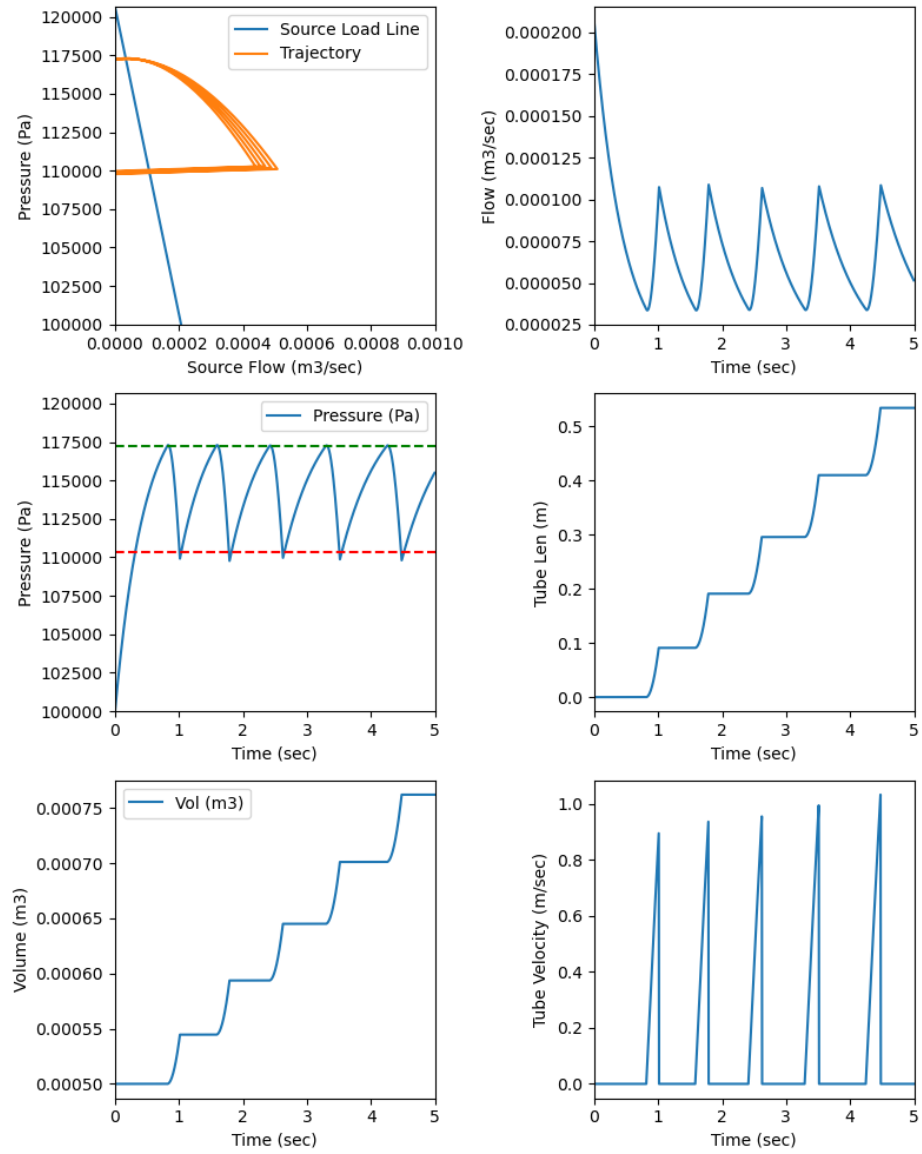


Figure 2: Simulation Run with approximate qualitative match. (See Lewis, Fig 9, hiI, hiTf)

Converting airflow (m^3/sec) to rate of molar mass flow:

$$\dot{N} = Fl_{source} \cdot \text{moles_per_m3} \quad (12)$$

Model velocity and length dependent eversion force which is resistance to pulling out eversion material:

$$F_D(L, \dot{L}) = 2LK_D\dot{L} \quad (13)$$

Where the factor of two accounts for everting material going at twice tube growth rate, \dot{L} .
Update length of crumpled material (if any)

$$L_C = \max(0, r\theta - L) \quad (14)$$

We have a switching model to replicate observed intermittent starting and stopping of eversion which updates the state based on current pressure:

$$\text{state} = \begin{cases} \text{GROWING}, & P > P2 \\ \text{unchanged}, & P1 \leq P \leq P2 \\ \text{STUCK}, & P < P1 \end{cases} \quad (15)$$

We are currently investigating changing this switching model to one based on thresholding net eversion force rather than tip surface pressure:

$$\text{state1} = \begin{cases} \text{GROWING}, & F_{ever} > F2 \\ \text{unchanged}, & F1 \leq F_{ever} \leq F2 \\ \text{STUCK}, & F_{ever} < F1 \end{cases} \quad (16)$$

In either case above, we update the crumple state as

$$\text{state2} = \begin{cases} \text{TAUGHT}, & L_C \leq 0 \\ \text{SLACK}, & L_C > 0 \end{cases} \quad (17)$$

Finally, we integrate the state variables:

$$\begin{aligned} \dot{L} &= \dot{L} + \ddot{L}dt \\ L &= L + \dot{L}dt \\ \dot{\theta} &= \dot{\theta} + \ddot{\theta}dt \\ \theta &= \theta + \dot{\theta}dt \\ N &= N + \dot{N}dt \end{aligned} \quad (18)$$

2.1 Initial Conditions

$$\begin{aligned} P &= 1 \text{ atmosphere} \\ \text{state1} &= \text{STUCK} \\ \text{state2} &= \text{TAUGHT} \\ N &= N(V_{housing} - V_{contents})/RT \\ L &= 0 \\ \dot{L} &= 0 \\ \ddot{L} &= 0 \end{aligned} \quad (19)$$

3 Simulation Results

4 Simplified Simulation Results

These initial results are from a simplified model assuming the TAUGHT state at all times. All parameters for the above model were computed from measurements of the experimental system with the

exception of `PBA_static`, `PHalt_dyn`, `Kdrag` which were estimated by a visual match to experimental data. Initial simulation results using the baseline parameters (Sec. 5, below) are given in Figure 2.

Some parameters were iteratively changed based on remaining observed differences between Figure 2 and experiment. Specifically:

Observation	Param	Original Value	Modified Value
Velocities too high	<code>Kdrag</code>	0.3	0.6
Pressure thresholds converge with time	<code>PBA_static</code>	$1.17 \times 10^5 \text{ Pa}$	$1.17 \times 10^5 - 500L \text{ Pa}$
Pressure thresholds converge with time	<code>PHalt_dyn</code>	$1.17 \times 10^5 \text{ Pa}$	$1.013 \times 10^5 + 500L \text{ Pa}$
Pressure rise too slow	$V_{housing}$	$0.5 \times 10^{-3} \text{ m}^3$	$0.05 \times 10^{-3} \text{ m}^3$
Peak Velocity too high	J	$5.10 \times 10^4 \text{ kg/m}^2$	$10.2 \times 10^4 \text{ kg/m}^2$

The modified parameter set is given in Section 6 below. Asterisks (*) denote iteratively changed parameters.

Simulation with the modified parameters (Figure 3) improve the model fit to data by 1) Shrinking loops on the pressure flow plot (upper left) are similar to shrinking loops in experimental pressure-velocity plot' 2) Convergence of the eversion thresholds (center left) causes the shrinking loops above, 3) Peak velocities better match peaks of fig. 9, and match the pattern of the highest velocity appearing near the center of travel. 4) With the modified parameters there are about 2 bursts per second, similar to the experimental rate.

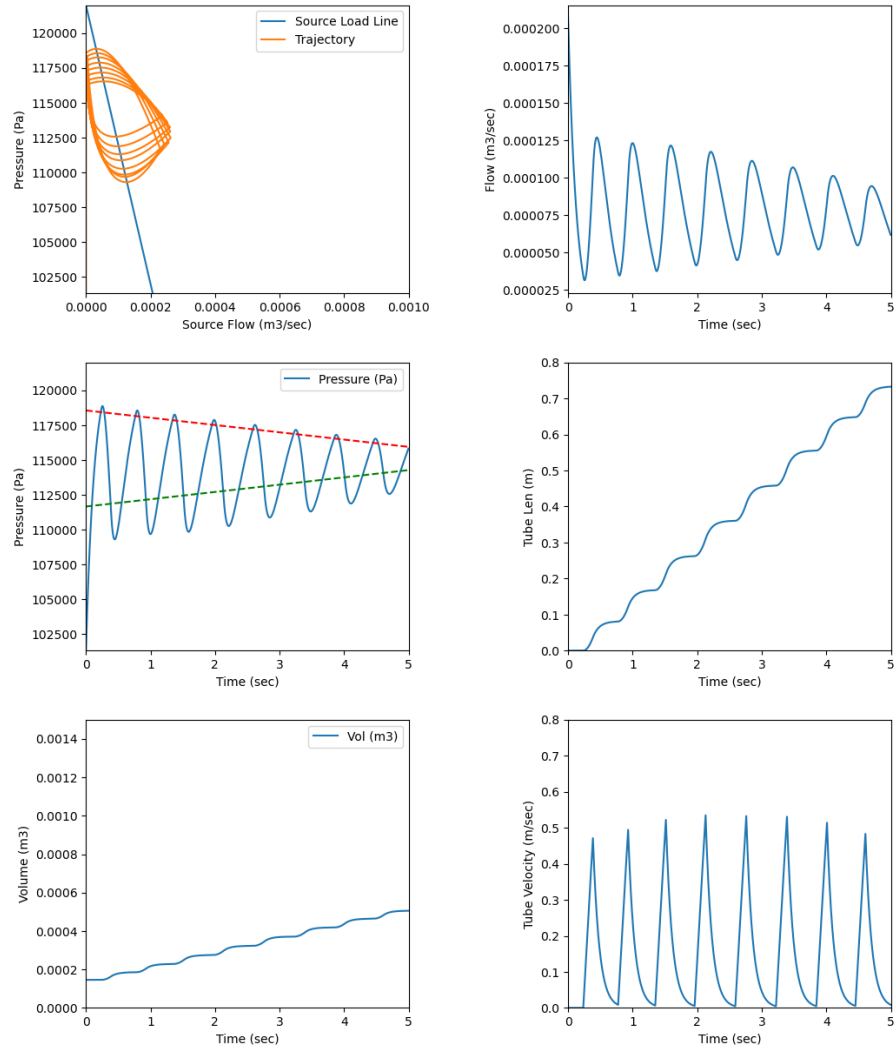


Figure 3: Improved qualitative match with modified parameters. (See Lewis, Fig 9, hiI, hiTf)

5 Baseline Parameter Values

moles_per_m3	4.4623E+01	moles / m3
Psource_SIu	1.2066E+05	Pascals
LLine_SIu	1.0000E-08	m3/sec / Pascal
Rsource_SIu	1.0000E+08	Pa/m3/sec
Vhousing_m3	1.4616E-03	m3
Kdrag	3.0000E-01	N / m2 / sec
area_m2	4.9087E-04	m2
Pintercept	1.2066E+05	Pascals
Fintercept	2.0684E-04	m3/sec
Vintercept	4.2137E-01	m/sec
PBA_static	1.1721E+05	Pascals
PHalt_dyn	1.1032E+05	Pascals
Patmosphere	1.0132E+05	Pascals

6 Modified Parameter Values

moles_per_m3	4.4623E+01	moles / m3 of Air
Patmosphere	1.0132E+05	Pascals
Psource_SIu	1.2201E+05	Pascals
LLine_SIu	1.0000E-08	m3/sec / Pascal
Rsource_SIu	1.0000E+08	Pa/m3/sec
J	* 1.0200E-03	kg/m2
Vhousing_m3	* 1.4616E-04	m3
Kdrag	* 1.2000E+00	N / m2 / sec
area_m2	4.9087E-04	m2
Pintercept	1.2201E+05	Pascals
Fintercept	2.0684E-04	m3/sec
Vintercept	4.2138E-01	m/sec
Threshold Taper	* 3.5714E+03	Pa /m
PBA_static	1.1856E+05	Pascals
PHalt_dyn	1.1167E+05	Pascals

7 Parameter Estimation from Data

The following process can be used to fit parameters to an eversion data record where the record consists of the following data as a function of time:

- Pressure in the tube storage chamber (Pa)
- Air flow from source into tube storage chamber (m^3/sec)
- Length of everting tube relative to chamber opening (m)
- Velocity of eversion (derived) (m/sec)

These can be plotted multiple ways such as in Fig 2 for example.

We can then use the following procedure to iteratively tune some of the model parameters to match a particular experimental run. Other parameters such as the tube reel radius, inertia, and braking friction are readily measured independently [?] and not fit to the eversion experiments.

- Adjust load line pressure intercept.

Data Focus: Pressure/Flow curves (upper left):

Procedure: Adjust Psource_SIu to move the load line and sim trajectory (they should overlap) up and down. Adjust Rsource_SIu to adjust its slope (higher values slope down more).

- Adjust stop-start thresholds.

Data Focus: Pressure-Time curves (middle left):

Procedure: Adjust PBA_static up or down to match the pressure peaks in experiment (green dashed).
Adjust PHalt_dyn up or down to match the pressure valleys.

- Adjust threshold taper.

Data Focus: Pressure-Time curves (middle left):

Procedure: Adjust Threshold Taper up or down to speed or slow down convergence of the thresholds.

- Adjust Friction or drag

Data Focus: Length-Time curves (middle right):

Procedure: Adjust the viscous drag constant of tubing (K_drag) up or down to match the overall slope of the data trace. Adjust max tubing length (Lmax) to match stopping point of data.

- Experiment with other parameters or go back and repeat the procedure.

8 Model Refinements

8.1 Varying tube profile

While most ET research uses tubing of constant diameter, the effective diameter of an ET can vary with length in two main ways. First, the tube can be fabricated with variable diameter by thermal welding of two sheets. Second, tubing of constant diameter may be everted into a tubular space of changing diameters. While the mechanics of eversion will in general be different in these two cases, we will initially ignore that difference and make tube diameter a function of eversion distance L , $V(L)$.

Tube profiles

Simulations

8.2 Multiple compartment model

So far, pressure and flow dynamics have considered the tubing supply chamber and the everted tubing to be a single compartment for computation of volume (Eqn 1) and pressure (Eqn 2) yielding a single flow (Eqn 11).

In some experimental data [...details...] we noted loops in the pressure-flow plane in which a growing ET deviated significantly from the source load line. This indicates that air pressure does not instantaneously equilibrate along the ET, but instead takes time to flow from the tubing compartment down to new volume at the growing tip. A lumped parameter model of this flow can be formed of two compartments, one is the reel housing from which the tube is everted, and the second is the tubing. A flow resistance, $R_T(L)$, connects the two chambers and this resistance increases with length. The tubing volume increases with length (as it did in Eqn 1).

Such a model is shown in Figure 4.

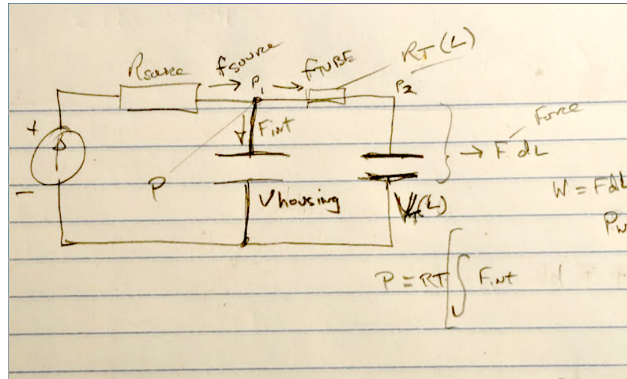


Figure 4: Two compartment, lumped parameter model.

We need to expand our model state variables as follows:

$$\begin{aligned}
N, \dot{N} &\rightarrow \{N_1, N_2, \dot{N}_1, \dot{N}_2\} \\
V_t &\rightarrow \{V_{housing}, V_T(L)\} \\
f_{source} &\rightarrow \{f_{source}, f_{int}, f_T\} \\
P &\rightarrow \{P_{C1}, P_{C2}\}
\end{aligned} \tag{20}$$

where N_1 and N_2 are the molar quantity of air in the housing and tube respectively, f_i are the respective flows indicated in Figure 4, and P_{C1} and P_{C2} are the pressures in the housing and tube respectively.

We then have new equations to replace or expand Equations 2, 11, and 12 as follows:

$$\dot{N}_1 = f_{source} - f_{int} - f_T \tag{21}$$

$$\dot{N}_2 = f_T \tag{22}$$

$$P_{C1} = \frac{N_1 RT}{V_{housing}} \tag{23}$$

$$P_{C2} = \frac{N_2 RT}{V_T(L)} \tag{24}$$

$$f_{source} = (P_{source} - P_{C1})/R_{source} \tag{25}$$

$$f_T = (P_{C1} - P_{C2})/R_T(L) \tag{26}$$

$$f_{int} = f_{source} - f_T \tag{27}$$

9 Results of Two Compartment Model

The data sets were simulated with the two-compartment version of the model. Volume of the ET was a function of length, L . Flow resistance between reel housing (compartment 1) and the ET was approximated by a ratio of R_{source_SIu} (typically 0.1).

Results from Tube 1, Trial 2 (hi inertia, hi friction) are given in Figure 5. Notably, the simulated tube pressure deviates below the source loadline during the start-stop oscillations similar to the experimental data.

References

- [1] Laura H Blumenschein, Allison M Okamura, and Elliot W Hawkes. Modeling of bioinspired apical extension in a soft robot. In *Conference on Biomimetic and Biohybrid Systems*, pages 522–531. Springer, 2017.
- [2] Panagiotis Vartholomeos, Zicong Wu, Hadi Sadati, and Christos Bergeles. Lumped parameter dynamic model of an eversion growing robot: Analysis, simulation and experimental validation. In *IEEE International Conference on Robotics and Automation (ICRA)*, 2024.

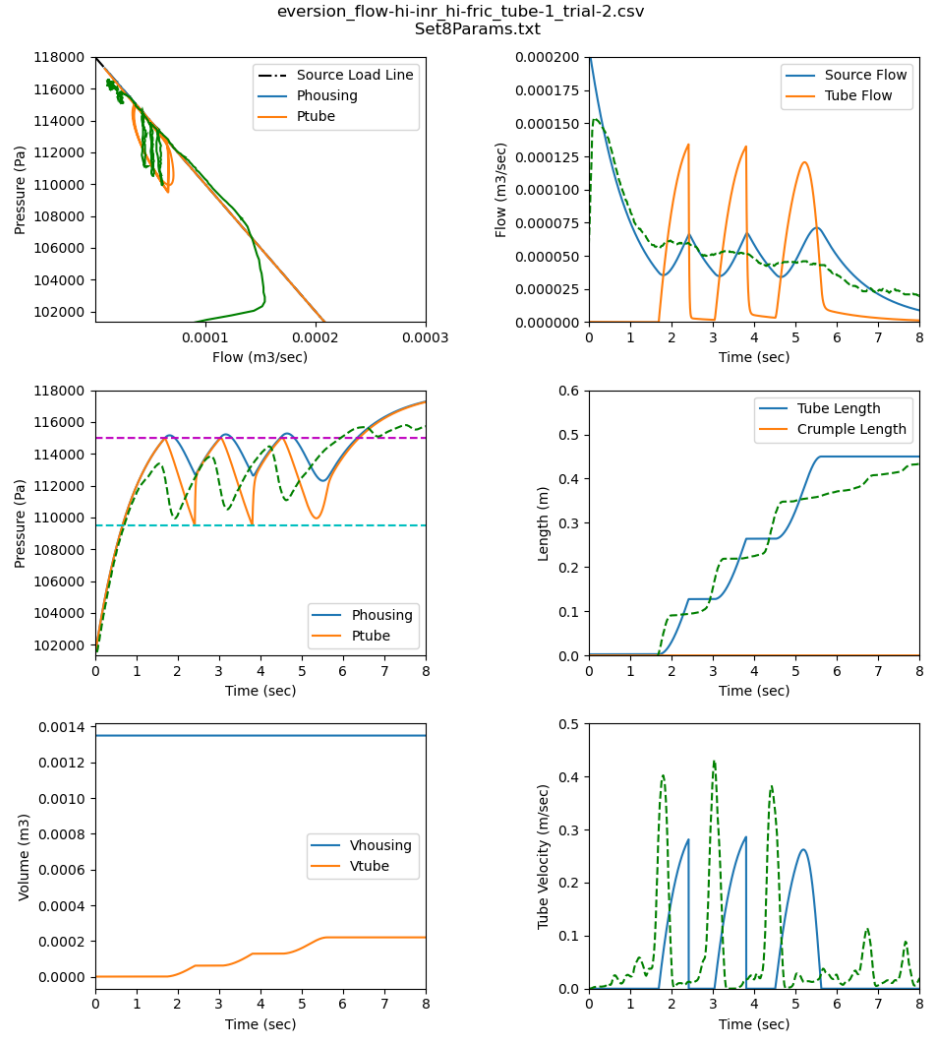


Figure 5: Two compartment model compared with simulation (See Lewis, Fig 9, hiI, hiTf)